


# Sperm fate is promoted by the *mir-44* microRNA family in the *Caenorhabditis elegans* hermaphrodite germline

Katherine A. Maniates, Benjamin S. Olson,<sup>†</sup> and Allison L. Abbott \*

Department of Biological Sciences, Marquette University, 1428 W. Clybourn Ave, PO Box 1881, Milwaukee, WI 53233, USA

<sup>†</sup>Present address: Division of Biology and Biomedical Sciences, Washington University, St. Louis, MO 63110, USA.

\*Corresponding author: Department of Biological Sciences, Marquette University, 1428 W. Clybourn Ave, PO Box 1881, Milwaukee, WI 53233, USA.  
allison.abbott@marquette.edu

## Abstract

Posttranscriptional regulation of gene expression, typically effected by RNA-binding proteins, microRNAs (miRNAs), and translation initiation factors, is essential for normal germ cell function. Numerous miRNAs have been detected in the germline; however, the functions of specific miRNAs remain largely unknown. Functions of miRNAs have been difficult to determine as miRNAs often modestly repress target mRNAs and are suggested to sculpt or fine tune gene expression to allow for the robust expression of cell fates. In *Caenorhabditis elegans* hermaphrodites, cell fate decisions are made for germline sex determination during larval development when sperm are generated in a short window before the switch to oocyte production. Here, analysis of newly generated *mir-44* family mutants has identified a family of miRNAs that modulate the germline sex determination pathway in *C. elegans*. Mutants with the loss of *mir-44* and *mir-45* produce fewer sperm, showing both a delay in the specification and formation of sperm as well as an early termination of sperm specification accompanied by a premature switch to oocyte production. *mir-44* and *mir-45* are necessary for the normal period of *fog-1* expression in larval development. Through genetic analysis, we find that *mir-44* and *mir-45* may act upstream of *fbf-1* and *fem-3* to promote sperm specification. Our research indicates that the *mir-44* family promotes sperm cell fate specification during larval development and identifies an additional posttranscriptional regulator of the germline sex determination pathway.

**Keywords:** *Caenorhabditis elegans*; microRNA; fertility; germline; sperm

## Introduction

Precise control of gene expression is essential for the specification of cell fates. Gene expression can be regulated at multiple levels including posttranscriptional regulation of mRNA stability and translation. Misregulation of key genes during development results in defects in processes such as germ cell development and specification (reviewed in Kimble and Crittenden 2007; Ellis 2008). In the *Caenorhabditis elegans* germline, gene expression is often controlled posttranscriptionally through the 3' UTR of mRNAs (Merritt et al. 2008). One class of posttranscriptional regulators is the set of small RNAs known as microRNAs (miRNAs) that act as small guide RNAs to repress translation, typically through binding to the 3' UTR of target mRNAs (reviewed in Ambros and Ruvkun 2018; Bartel 2018). Reduced miRNA biogenesis activity results in germline defects along with reduced fertility or sterility (Grishok et al. 2001; Denli et al. 2004; Bukhari et al. 2012; Brown et al. 2017; Rios et al. 2017).

While numerous individual miRNAs have been detected in the germline (McEwen et al. 2016; Minogue et al. 2018; Bezler et al. 2019), the functions of germline miRNAs remain largely unknown. Identification of functions of miRNAs has been difficult to determine as miRNAs often modestly repress target mRNAs and are suggested to sculpt or fine tune gene expression to allow

for the robust expression of cell fates. Thus, many miRNA loss-of-function mutants do not have easily observable mutant phenotypes (Miska et al. 2007; Alvarez-Saavedra and Horvitz 2010). One family of miRNAs with well-described germline functions is the *mir-35* family. The *mir-35* family acts in the germline and soma to regulate fecundity and embryonic development, specifically in the process of sex determination in the developing embryo (McJunkin and Ambros 2014, 2017).

We sought to understand the function of another family of miRNAs that are also expressed in the germline, the *mir-44* family. The *mir-44* family is made up of four miRNAs, *mir-44*, *mir-45*, *mir-61*, and *mir-247*, that share the same seed sequence (Figure 1A). Three family members are found in genomic clusters with other miRNAs: *mir-44* is in a cluster with *mir-42* and *mir-43*, *mir-61* is in a cluster with *mir-250*, and *mir-247* is in a cluster with *mir-797* (Figure 1B). *mir-43*, *mir-250*, and *mir-797* are all members of the *mir-2* family (Ruby et al. 2006). Prior studies have shown that the *mir-44* family of miRNAs is expressed in a diverse set of somatic cells and tissues including the intestine (*mir-42/44*; *mir-45*), vulva (*mir-42/44*; *mir-61*), seam cells (*mir-42/44*), pharynx (*mir-45*; *mir-247*), head muscle (*mir-42/44*; *mir-45*), and distal tip cell (*mir-247*) (Martinez et al. 2008). In addition, three *mir-44* family members, *mir-44*, *mir-45*, and *mir-61*, are expressed in both male and hermaphrodite gonad arms (Minogue et al. 2018; Bezler et al.

Received: October 16, 2020. Accepted: November 12, 2020

© The Author(s) 2020. Published by Oxford University Press on behalf of Genetics Society of America. All rights reserved.

For permissions, please email: journals.permissions@oup.com

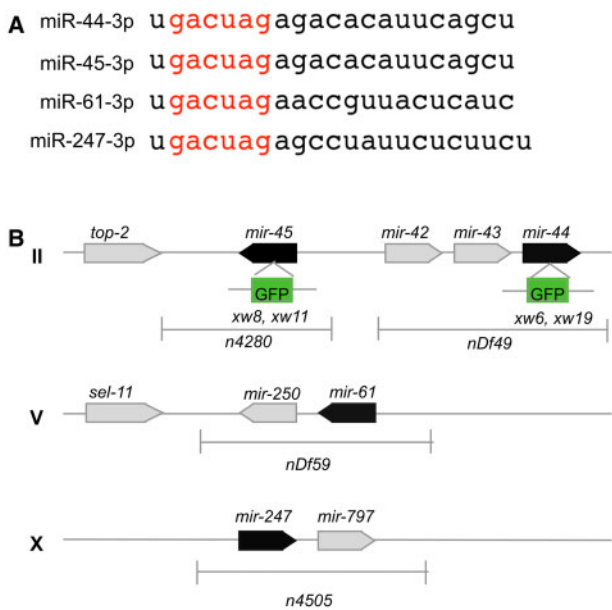


**Figure 1** miR-44 family sequences and allele information. (A) Mature sequences of miR-44 family members. miR-44 family members are grouped together based on their shared seed sequence (red). (B) Cartoon to show genomic location of miR-44 family genes (black) with clustered unrelated miRNA genes and protein coding genes (gray). Allele information is listed under each locus.

2019), though appear to found at higher levels in the hermaphrodite gonads (Bezler et al. 2019). miR-247 expression is also detected in gonad arms but at a much lower level (Minogue et al. 2018; Bezler et al. 2019). miR-61 is expressed in germ cells from the late pachytene stage to maturing oocytes in adult hermaphrodites (Minogue et al. 2018).

The miR-44 family in *C. elegans* is part of the larger evolutionarily conserved miR-279 family, members of which are found in many diverse animals including worms and insects (Fromm et al. 2015, 2020). In *Drosophila*, miR-279 regulates Apontic, which functions to define cell fates in the ovarian follicle cells and somatic stem cells in the testes via regulation of STAT signaling (Yoon et al. 2011; Monahan and Starz-Gaiano 2016). miR-279 also regulates cell fates in the *Drosophila* eye (Duan et al. 2018). In *C. elegans*, mutants of multiple members of the miR-44 family have complex defects in egg laying (Alvarez-Saavedra and Horvitz 2010). In addition, miR-61 targets *vav-1* during Notch signaling in vulval development (Yoo and Greenwald 2005). However, no germline functions have yet been identified for the miR-44 family in *C. elegans*.

Importantly, as mutants missing both miR-44 and miR-45 had not been generated due to their close proximity in the genome, analysis of the miR-44 family in *C. elegans* has remained incomplete. Analysis of mutants missing both miR-44 and miR-45 is critical because the mature miRNA sequences for miR-44 and miR-45 are identical (Lau et al. 2001). To address this, we have generated new deletion alleles to address the function of miR-44 family members. Our work has identified a function for the miR-44 family of miRNAs in the regulation of the germline sex determination pathway during larval development.

In *C. elegans* hermaphrodites, cell fate decisions for germline sex determination are made during larval development, when sperm are generated in a short temporal window before the switch to oocyte production (Ellis and Schedl 2007; Kimble and Crittenden 2007; Ellis 2008). The regulators of germline sex

determination are under tight control to specify the correct number of sperm since too many or too few sperm decreases the fitness of the animal (Hodgkin and Barnes 1991). Control of germline sex determination is modulated by several classes of posttranscriptional regulators: RNA-binding proteins, miRNAs, and translation initiation factors. Misregulation of these factors can improperly specify sperm or oocyte fate and affect the number of germ cells specified (Amiri et al. 2001; Bachorik and Kimble 2005; Huggins et al. 2020 and reviewed in Kimble and Crittenden 2007). FOG-1 and FOG-3 function at the terminal end of the germ cell specification pathway to promote spermatogenesis and repress oogenesis (reviewed in Kimble and Crittenden 2007; Ellis 2008). Precise control of *fog-1* and *fog-3* regulates the specification of germ cells as sperm (Barton and Kimble 1990; Chen and Ellis 2000; Lamont and Kimble 2007). Levels of FOG-1 and FOG-3 proteins are regulated in part by the repressors TRA-1 and FEM-3. Both the *fog* genes and *fem-3* are repressed by *fbf-1* and *fbf-2* posttranscriptionally (Ahringer and Kimble 1991; Zhang et al. 1997). The combination of the activities of the *fbf* and *fem* genes acts to coordinate the period and levels of *fog-1* and *fog-3*. A shortened length of FOG-1 expression or a reduced level of FOG-1 expression can decrease the number of sperm that are generated in hermaphrodites (Thompson et al. 2005; Lamont and Kimble 2007).

Here, we report that loss-of-function mutations in miR-44 and miR-45 are sufficient to significantly decrease the number of sperm generated in *C. elegans* hermaphrodites. Consistent with this, we find that miR-45 is expressed in the germline during the time of sperm specification. Sperm produced in miR-45(*xw11*) miR-42/44(*nDf49*) and miR-45(*xw8*) miR-44(*xw19*) mutants appear fully functional since the number of sperm generated closely correlates with the number of progeny produced. In addition, miR-44 and miR-45 are dispensable for sperm formation in males. Our data indicate that miR-44 and miR-45 regulate the period of sperm specification and the onset of oogenesis. Moreover, analysis of genetic interactions with germline sex determination regulators supports a model that miR-44 and miR-45 promote sperm specification through the regulation of *fbf-1* and *fem-3* to allow for normal *fog-1* expression. Our research indicates that the miR-44 family promotes the sperm cell fate decision during larval development.

## Methods

### *C. elegans* culture conditions

*C. elegans* strains were grown on NGM plates seeded with *Escherichia coli* strain AMA1004 at 20°C unless otherwise specified (Casadaban et al. 1983). Some strains were provided by the *Caenorhabditis* Genetics Center (CGC), which is funded by the NIH Office of Research Infrastructure Programs (P40 OD010440).

### Strain construction

For building multiply mutant strains, the presence of miRNA deletion alleles in F2 progeny was identified by performing PCR with primers that amplify the genomic region flanking the deletion mutation or insertion. Sequences for primers used for genotyping are found in Supplementary Table S1. Strains built with *fog-1*(*q253*) and *fem-3*(*q20*) alleles, which are point mutations, were confirmed by sequencing. For CRISPR-Cas9 genome editing, plasmids pJW1219 (Addgene plasmid # 61250) and pDD282 (Addgene plasmid # 66823) were used (Dickinson et al. 2015; Ward 2015). A short guide RNA to target Cas9 to the endogenous miR-45 locus was designed and cloned into pJW1219. A homologous

recombination template to replace 60 nucleotides of the *mir-45* stem loop sequence with a GFP insertion was cloned into pDD282. The *mir-44* modification was designed using the same method to replace 100 nucleotides of the *mir-44* sequence with a GFP insertion. Sequencing information for all CRISPR-generated alleles is described in Supplementary Table S1. Plasmids for CRISPR-Cas9 genome editing were injected into wild-type worms, *mir-42/44*(nDf49), or *mir-45*(*xw8*) mutants. Selectable markers were used to identify successful genome modifications based on published protocols (Dickinson et al. 2015). Loss of *mir-45* was further confirmed by PCR and sequencing. A list of all strains is in Supplementary Table S2.

### Antibody staining MAPK staining

Young adult worms were dissected to release gonad arms, fixed, and blocked (Gervaise and Arur 2016). The anti-activated MAP kinase antibody (dpERK, Sigma, M9692) was used at a 1:400 dilution to detect diphosphorylated MAPK using the indirect immunofluorescence. Dissected gonads were then incubated with Alexa Fluor 555 goat anti-mouse secondary antibody (Fisher, A28180).

### SPE-44, FOG-1, and GFP expression analysis

Worms were synchronized and then picked during the lethargus period at the L2 molt (L2m), L3 molt (L3m), or L4 molt (L4m) stage and transferred to a new plate until the indicated time: mid-L3 (L2m + 3 h), late L3 (L2m + 9 h), mid-L4 (L3m + 4 h), mid-late L4 (L3m + 7 h), or young adult (L4m + 2 h). The worms were then dissected to release the gonad arms, freeze cracked, fixed with 3% paraformaldehyde in potassium phosphate buffer, and blocked with 3% normal goat serum (Crittenden and Kimble 2006; Gervaise and Arur 2016). The anti-Myc 9E10 antibody (Santa Cruz Biotechnology, sc-40) was used at a 1:50 dilution to detect *qSi140* [*3xMyc::fog-1*] in a *fog-1*(*q785*) background and then detected with Alexa Fluor 555 goat anti-mouse secondary antibody (Fisher, A28180). The anti-SPE-44 antibody (Gift from Harold Smith, described in Kulkarni et al. 2012) was used at a 1:100 dilution to detect SPE-44 and then detected with Alexa Fluor 488 donkey anti-rabbit secondary antibody (Invitrogen, A-21206). The rabbit anti-GFP antibody (Novus, NB600-308) and Alexa Fluor 488 donkey anti-rabbit secondary antibody (Invitrogen, A-21206) were used to detect GFP in *mir-44*(*xw6*[*gfp*<sup>3xFlag</sup>]) II and *mir-45*(*xw8*[*gfp*<sup>3xFlag</sup>]) II worms.

### Imaging

Nomarski DIC and epifluorescence microscopy was performed using a Nikon 80i compound microscope. Images were taken using a CoolSNAP HQ2 monochrome camera (Roper Scientific). Images were captured with a 60× Plan Apo objective lens and analyzed using Nikon Elements software. Expression analysis of worms with the *xw8* allele, which has *gfp* inserted into the *mir-45* endogenous locus, was performed using a Nikon Inverted Microscope Eclipse Ti-E confocal microscope at 60×.

### RT-qPCR

A total of 100 young adult hermaphrodites were placed into TRIzol, flash frozen in liquid nitrogen, and stored at -80°C until use. RNA was extracted using Direct-Zol RNA MicroPrep (Zymo Research) according to manufacturer's directions. MicroRNA TaqMan PCR assays (Applied Biosciences/ThermoFisher) were performed following manufacturer's directions. Analysis of U18, a snoRNA, was used to normalize RNA levels between samples. The following TaqMan assays were used U18 (ThermoFisher

Assay ID 001764), *miR-42* (ThermoFisher Assay ID 241800\_mat), *miR-43* (ThermoFisher Assay ID 000204) *miR-44* (ThermoFisher Assay ID 000205), *miR-35* (ThermoFisher Assay ID 462881\_mat), *let-7* (ThermoFisher Assay ID 000377), and *miR-58* (ThermoFisher Assay ID 000216). A total of three independent biological samples were analyzed, each with three technical replicates. Analysis of qPCR was done as described in Livak and Schmittgen (2001) by comparing  $\Delta\Delta Ct$  values.

### Phenotype analysis Brood size and unfertilized oocytes

To assess brood size, an individual L4 stage worm was placed on a seeded plate and transferred to a new plate every 24 h for 4 days. All larval progeny were counted on each plate to determine total brood size, dead embryos were not scored. Embryonic lethality was scored independently. Unfertilized oocytes were determined in two ways. First, for all strains in Supplementary Table S3, the total number of unfertilized oocytes produced was counted for the entire reproductive life of an individual worm. For this assay, an individual L4 stage worm was placed on a seeded plate and transferred to a new plate every 24 h for 4 days, and the total number of unfertilized oocytes, embryos, and live progeny was counted for individual hermaphrodites. Second, the number of unfertilized oocytes was counted in a defined time period in 2-day-old adults to compare the number of unfertilized oocytes that are produced between strains. For this assay, which was used to assess the rate of unfertilized oocytes produced after mating with males, one hermaphrodite was placed with one RF963 (*oxTi302* [*eft-3p::mCherry::tbb-2* 3'UTR + *Cbr-unc-119*(+)] I; *him-8*(*e1489*) IV) male for 24 h and allowed to mate. Any hermaphrodites that produced mCherry-positive progeny were analyzed by counting the number of unfertilized oocytes produced on the second and third days of the assay. For both assays, the percent Unfertilized Oocytes was calculated for each worm: [(total # unfertilized oocytes)/(total # fertilized embryos + hatched worms + unfertilized oocytes)] × 100.

### Adult lethality

To determine the penetrance of adult lethality, we measured the bagging phenotype caused by internally hatching progeny and the bursting at the vulva phenotype. A total of 20 L4-stage hermaphrodites were transferred to a new NGM plate each day. Surviving worms were transferred each day, and the number of bagged worms and worms that burst through the vulva on each plate was counted for 3 days.

### Embryonic lethality

Embryonic lethality was quantified by transferring embryos to a seeded NGM plate and counting the number of unhatched embryos 24 h later. The percent embryonic lethality was calculated by dividing the number of unhatched embryos by the total number of embryos.

### Ovulation rate

Oocyte maturation rates were determined by counting the number of fertilized oocytes in a 3-h time period in the uterus and on the plate (McCarter et al. 1999). The rate assesses the number of embryos that are produced during this time period taking into account the initial and final number of embryos in both the uterus and laid on the plate. The following equation was used for this calculation: ovulation rate per gonad arm per hour = (# embryos in uterus after 3 h + # progeny on plate) - (# embryos initially in uterus)/(2 gonad arms per animal × 3 h assay). To test the effect

of exogenous male sperm on ovulation rate, L4-stage hermaphrodites and L4-stage males (expressing *his-72::gfp* transgene) were placed together in a 1:5 ratio onto a seeded NGM plate overnight. After mating overnight, the maturation rate was calculated for 3 h. Hermaphrodites were then examined for the presence of GFP sperm to confirm the successful mating and transfer of sperm.

### Sperm quantification

Sperm were quantified using the *his-72::gfp* transgene (Huang et al. 2012). Individual worms were placed on a coverslip in a 4- $\mu$ l drop of sperm buffer and then smashed by placing the coverslip on a slide to count the sperm using epifluorescence microscopy on a compound microscope. Hermaphrodites were assayed at L4m + 4 h, and males were assayed at L4m + 10 h. Strains containing the *fem-3(q20)* allele did not exhibit detectable *his-72::gfp* expression. Therefore, DAPI staining was used to quantify sperm. DAPI staining was also used to quantify sperm in the strains (Supplementary Table S3). For this, young adults prior to first ovulation event were frozen in methanol at  $-20^{\circ}\text{C}$  for at least 1 hour, washed, placed on a cover slip, with 2  $\mu$ l of Vectashield with DAPI, then smashed on a slide, and counted similarly to the *his-72::gfp* sperm counting.

### Appearance of first embryos

Hermaphrodites were analyzed at 3.75 h post-L4 molt at  $25^{\circ}\text{C}$ , 5 h post-L4 molt at  $20^{\circ}\text{C}$ , and 7.5 h post-L4 molt at  $15^{\circ}\text{C}$  based on published growth parameters (Byerly et al. 1976). The presence of oocytes and the number of embryos were counted for at least 15 worms per strain.

### Appearance of sperm

Hermaphrodites were analyzed at mid-L4 (L3m + 4 h), mid-late L4 (L3m + 7 h), late L4 (L3m + 10 h), and L4 molt. The presence of GFP in the condensed nuclei typical of haploid spermatids was analyzed using *his-72::gfp* transgene. The expression of *his-72::gfp* was assessed for at least 10 worms per strain.

### Developmental progression to the L4 stage

To measure the timing of developmental progression, 100 L1 animals were placed on a seeded NGM plate following synchronization by bleaching. The number of worms that were at the L4 molt stage 48 h after placement on plate was determined by the observation of vulva morphology and observations of worms in the lethargus state.

### Sterility and Mog phenotype

Masculinization of germline (Mog) phenotype was assessed as described in Barton et al. (1987): single L4 stage hermaphrodites were scored for the presence of any embryos on the plate. After 3 days, any worms that did not produce embryos were categorized as sterile. Additional assays were performed examining worms for the presence of oocytes after 3 days and worms that failed to produce oocytes were categorized as Mog.

### Gene ontology analysis of computationally predicted targets

Computationally predicted targets of the *mir-44* family were identified using Target Scan Worm 6.2 (Lewis et al. 2005), any terms with a probability of conserved targeting (PcT; Friedman et al. 2008) of  $>0.1$  were then cross-referenced with germline-expressed genes (Tzur et al. 2018) to generate a set of candidate target mRNAs that were expressed in the hermaphrodite germline. DAVID 6.8 was then used to identify significantly

overrepresented functional annotations (Huang et al. 2009) with an EASE score  $P$ -value of  $>0.05$ .

### Quantification and statistical analysis

One-way ANOVA followed by either a Tukey *post hoc* test or Dunnett's multiple comparisons were performed using Graphpad Prism version 8.0.2 unless otherwise noted in the figure legend.

### Data availability

Strains and plasmids are available upon request. Strains that contain newly generated alleles for *mir-44* or *mir-45* (*xw6*, *xw8*, *xw11*, and *xw19*) are available at the CGC. The authors affirm that all data necessary for confirming the conclusions of the article are present within the article, figures, and tables.

Supplementary material is available at figshare DOI: <https://doi.org/10.25386/genetics.13103411>.

## Results

### Generation of deletion alleles for analysis of *mir-44* family function

We set out to investigate the functions of the *mir-44* family of miRNAs, which is composed of four miRNAs, *mir-44*, *mir-45*, *mir-61*, and *mir-247* (Lau et al. 2001; Lim 2003; Ruby et al. 2006; Figure 1A). Three of the *mir-44* family members are found in polycistronic clusters with miRNAs from other families. The *mir-44* and *mir-45* genes are located within 9 kb of each other on chromosome II (Figure 1B). Therefore, mutants missing both *mir-44* and *mir-45* were not generated in earlier analysis of miRNA families (Alvarez-Saavedra and Horvitz 2010). This is critical, particularly because the mature miRNA sequences for *mir-44* and *mir-45* are identical (Lau et al. 2001). To perform functional analysis on worms missing all *mir-44* family members, we used CRISPR/Cas9 to create a *mir-45* loss-of-function, *xw11*, mutation in a *mir-42/43/44* (*nDf49*) genetic background (Figure 1B). Conversely, we also generated a *mir-44* loss-of-function allele, *xw19*, in a *mir-45* (*xw8*) mutant background. The two CRISPR-Cas9-generated alleles *xw11* and *xw8* were created to delete the mature miRNA sequence for *mir-44* and *mir-45*, respectively, and also to insert GFP for use as transcriptional reporters.

### The *mir-44* family of miRNAs regulates hermaphrodite fecundity

We initially observed that *mir-44* family mutants had reduced brood sizes. Quantification of total brood size was performed for the full collection of *mir-44* family single and multiply mutant strains. It was observed that all *mir-44* family mutants had a brood size significantly lower than N2 wild-type worms (Figure 2A and Supplementary Table S3). All *mir-44* family mutants have low levels of embryonic lethality and some *mir-44* family multiply mutant strains show adult lethality from the bag of worms or bursting at the vulva phenotypes (Supplementary Table S3). We also noticed an increased number of unfertilized oocytes laid by *mir-44* family multiply mutant worms (Supplementary Table S3). For most phenotypes analyzed, there were some additive effects from losing additional *mir-44* family members, but these effects were modest. *mir-44* and *mir-45* have identical mature miRNA sequences and therefore have the ability to bind and repress the same target mRNAs. Because the strains missing these two identical family members represented a simple genetic background that resulted in strong fecundity defects, we chose to focus further functional analysis on mutants with the loss of *mir-44* and *mir-45*.



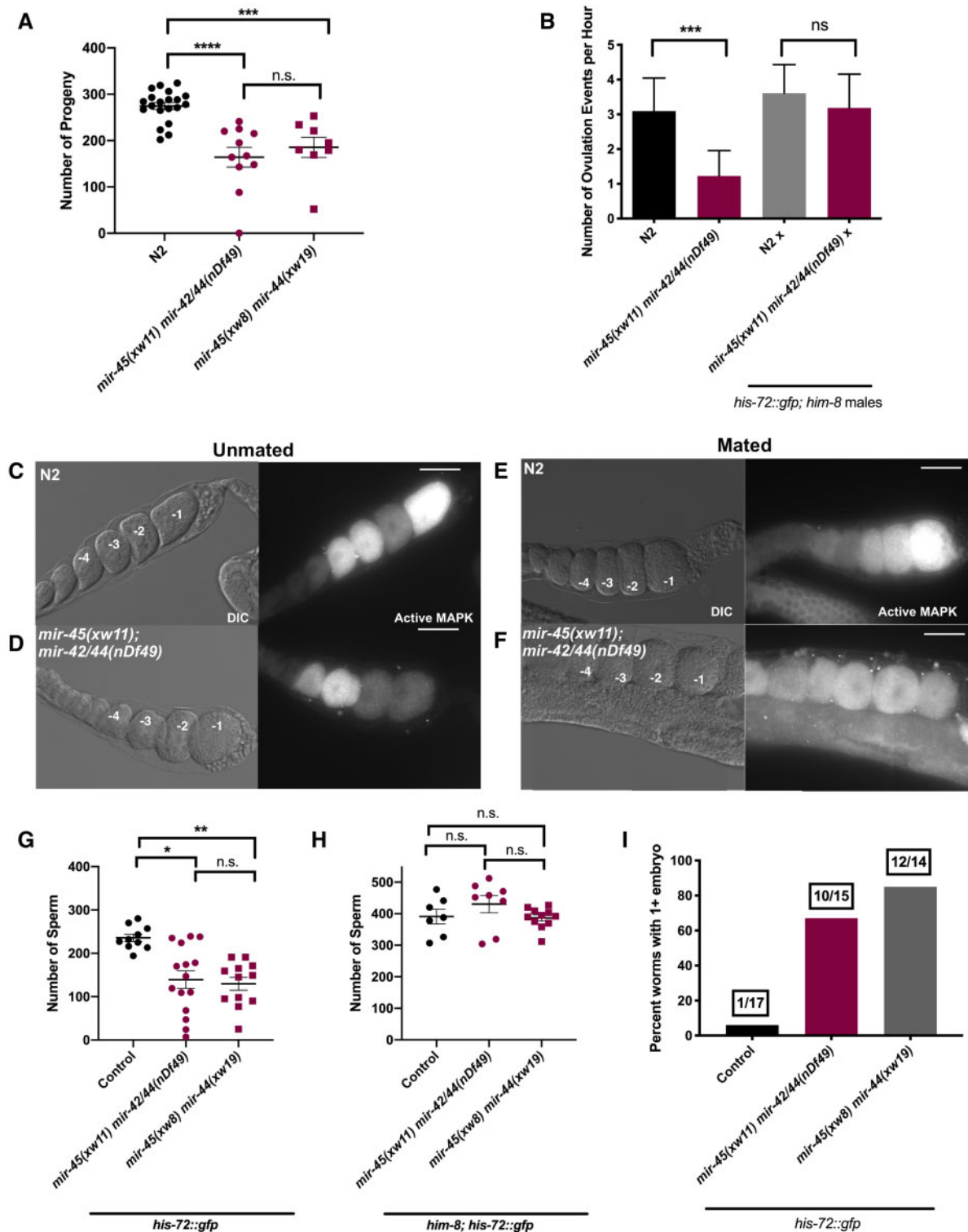


**Figure 2** Mutants with the loss of *mir-44* and *mir-45* have fecundity and sperm defects. (A) Quantification of total brood size of N2 control, *mir-45(xw11) mir-42/44(nDf49)* and *mir-45(xw8) mir-44(xw19)* worms ( $n \geq 8$  worms for each strain). (B) Ovulation rates (events/hour) were measured in N2 and *mir-45(xw11) mir-42/44(nDf49)* mutants. Hermaphrodites were mated with *him-8; his-72::gfp* males overnight to assess ovulation rate after mating ( $n \geq 20$ ). (C–F) Dissected adult hermaphrodite gonad arms analyzed with DIC microscopy or fluorescent microscopy using an antibody for diphosphorylated MAP Kinase (“Active MAPK”). (C and E) N2 worms and (D and F) *mir-45(xw11) mir-42/44(nDf49)* either unmated (C and D) or mated overnight with *his-72::gfp; him-8* males (E and F). Numbers denote proximal oocytes. Scale bars equal 25  $\mu\text{m}$ .  $n = 10$  gonad arms analyzed in each group. (G) Quantification of sperm in individual hermaphrodites at L4m + 5 h ( $n \geq 10$  for each strain). All strains have *his-72::gfp (stIs10027)* in the background. (H) Quantification of sperm in males at L4m + 10 h ( $n \geq 7$  for each strain). All strains have *him-8(e1489); his-72::gfp(stIs10027)* in the background. (I) Percentage of worms with one or more embryos at L4m + 5 h timepoint. Numbers above bars indicate the number of worms observed with one or more embryos over the total number analyzed. All strains have *his-72::gfp (stIs10027)* in the background. For graphs in (A), (G), and (H), each marker represents data for a single worm with a line indicating average  $\pm$  SEM. One-way ANOVA followed by Tukey post hoc test: \* $P < 0.05$ , \*\* $P < 0.01$ , \*\*\* $P < 0.001$ , \*\*\*\* $P < 0.0001$ , n.s. indicates  $P > 0.05$ .

The previously isolated allele for *mir-44*, *nDf49*, also lacked the other two miRNA genes in the *mir-42/44* cluster, *mir-42* and *mir-43*. Since *mir-42* is a member of the *mir-35* family, which has known fertility defects (McJunkin and Ambros 2014, 2017), it was possible that the observed fertility defects in *mir-45(xw11) mir-42/44(nDf49)* were due to the loss of *mir-42* activity. In contrast, *mir-45(xw8) mir-44(xw19)* has CRISPR-Cas9-generated deletion alleles that remove only the *mir-44* and *mir-45* miRNA sequences. Interestingly, *mir-45(xw11) mir-42/44(nDf49)* and *mir-45(xw8) mir-44(xw19)* strains displayed similar average brood sizes ( $164.2 \pm 70.5$ ,  $n = 11$  and  $179.2 \pm 60.4$ ,  $n = 9$ , respectively, Figure 2A and Supplementary Table S3), despite *mir-45(xw8) mir-44(xw19)* retaining intact *mir-42* and *mir-43* sequences. To confirm that *mir-42* and *mir-43* were expressed in *mir-45(xw8) mir-44(xw19)* mutants, RT-qPCR assays were performed to examine the levels of miR-42 and miR-43. Surprisingly, it was observed that both miR-42 and miR-43 levels were increased 24-fold and 33-fold, respectively, in *mir-45(xw8) mir-44(xw19)* mutants compared to the wild-type control, while in *mir-45(xw11) mir-42/44(nDf49)* mutants, miR-42 and miR-43 were not significantly increased. miRNAs not in the *mir-42/44* cluster, including *let-7*, *miR-35*, or *miR-58*, did not show an increase in mature miRNA levels (Supplementary Figure S1A). This indicates that the loss of *mir-42* activity is not responsible for the observed fecundity defects.

We next performed assays to determine if the observed low brood size (Figure 2A and Supplementary Table S3) and high number of unfertilized oocytes (Supplementary Table S3) phenotypes in mutants missing *mir-44* and *mir-45* were due to defects in sperm or in oocytes. We measured ovulation rate, a measure of how often oocytes undergo meiotic maturation and transit through the spermatheca (McCarter et al. 1999; Miller et al. 2003), which requires signaling from sperm and the proximal oocyte's ability to receive the signals to exit meiotic arrest and promote ovulatory sheath contractions (Greenstein 2005). The rate of ovulation was significantly decreased in *mir-45(xw11) mir-42/44(nDf49)* mutants compared to N2 wild-type worms (Figure 2B). This defect was not observed when *mir-45(xw11) mir-42/44(nDf49)* mutant hermaphrodites were mated with *his-72::gfp*; *him-8* control males, indicating that *mir-45(xw11) mir-42/44(nDf49)* oocytes can respond normally to exogenous sperm (Figure 2B). In addition, we found that mating *mir-45(xw11) mir-42/44(nDf49)* hermaphrodites with *oxTi302*; *him-8* males, which express an mCherry transgene, resulted in a suppression of the unfertilized oocyte phenotype in *mir-45(xw11) mir-42/44(nDf49)* mutants (Supplementary Figure S1B), indicating that oocyte defects are not the cause of the unfertilized oocyte phenotype.

To molecularly characterize the *mir-45(xw11) mir-42/44(nDf49)* mutant oocytes' response to sperm, we examined levels of active MAP kinase in *mir-45(xw11) mir-42/44(nDf49)* mutants relative to N2 controls (Figure 2C–F). MAP kinase normally increases in the proximal-most oocyte (–1 oocyte) to promote meiotic maturation in unmated N2 hermaphrodites and in the –2 oocyte following mating with males (Figure 2C and E; Miller et al. 2003; Lee et al. 2007; Gervaise and Arur 2016). *mir-45(xw11) mir-42/44(nDf49)* mutants showed decreased levels of active MAP kinase in the proximal-most oocyte (Figure 2D), which was not observed following mating of *mir-45(xw11) mir-42/44(nDf49)* mutants with control (*his-72::gfp*; *him-8*) males (Figure 2F). Together, these results indicate that mutants with the loss of *mir-44* and *mir-45* likely have sperm defects that can lead to reduced MAP kinase activation in proximal oocytes, a reduced rate of ovulation, and a

failure of successful fertilization leading to the unfertilized oocytes and reduced brood size.

### ***mir-44* and *mir-45* regulate the number of sperm produced in hermaphrodites**

To determine if the observed fecundity defects are due to a reduced number of sperm, we counted haploid spermatids in adult hermaphrodites in control and mutant worms with the loss of *mir-44* and *mir-45*, *mir-45(xw11) mir-42/44(nDf49)*, and *mir-45(xw8) mir-44(xw19)*, using a *his-72::gfp* transgene, *stIs10027*. The average number of spermatids was significantly decreased in *mir-45(xw11) mir-42/44(nDf49)* and *mir-45(xw8) mir-44(xw19)* mutant strains ( $139 \pm 78$ ,  $n = 15$  and  $130 \pm 52$ ,  $n = 12$ , respectively) compared to the control *his-72::gfp* (*stIs10027*) worms ( $235 \pm 27$ ,  $n = 10$ , Figure 2G). This reduction in sperm number appears to be specific to hermaphrodites; mutant males with the loss of *mir-44* and *mir-45* do not generate significantly fewer sperm (Figure 2H). However, mutant males with the loss of *mir-44* and *mir-45* have other defects in spermiogenesis and defects in the transfer of sperm to hermaphrodites (data not shown). Interestingly, the number of sperm produced in hermaphrodites (Figure 2G) closely correlated with the number of progeny determined in the brood size analysis (Figure 2A), indicating that sperm from hermaphrodites that lack *mir-44* and *mir-45* are functional and capable of maturing and successfully fertilizing oocytes. In addition, both mutant strains with the loss of *mir-44* and *mir-45* developed at the same rate as N2 wild-type worms (Supplementary Figure S1C), indicating that the defect in sperm production in hermaphrodites was not due to delayed or abnormal larval developmental progression.

### ***mir-44* and *mir-45* regulate the timing of sperm formation in hermaphrodites**

A reduced number of sperm can result from a premature termination of sperm specification leading to an early transition to oocyte production in the larval germline and subsequent early production of embryos in young adult worms. It could also reflect a delay or reduced rate of sperm specification, possibly with a normal timing of oocyte and embryo production (Barton and Kimble 1990; Lamont and Kimble 2007). To test this, we looked at worms 5 h after the L4 molt, a period in which sperm production is typically finished, but embryo production has not yet begun in wild-type worms. We found that 66% (10/15) of *mir-45(xw11) mir-42/44(nDf49)*; *his-72::gfp* mutants and 86% (12/14) of *mir-45(xw8) mir-44(xw19)*; *his-72::gfp* mutants had embryos at this time compared to 6% (1/17) of *his-72::gfp* worms (Figure 2I).

To analyze the timing of sperm specification in the loss-of-function *mir-44* and *mir-45* mutants, we looked for the appearance of spermatids using the *his-72::gfp* transgene at different timepoints during the L4 stage. Spermatids were identified by their characteristic condensed nuclei. At the mid-late L4 stage, 81% (13/16) of *his-72::gfp* control worms had spermatids formed whereas only 18% (3/17) of *mir-45(xw11) mir-42/44(nDf49)* mutants and 19% (3/16) of *mir-45(xw8) mir-44(xw19)* mutants started spermatogenesis at this same time point (Figure 3A and Supplementary Figure S2A). At the late L4 stage, 3 h later, 93% (14/15) of *his-72::gfp* control worms had spermatids detected; however, only 66% (10/15) of the *mir-45(xw11) mir-42/44(nDf49)* mutants and 69% (9/13) of the *mir-45(xw8) mir-44(xw19)* mutants had detectable spermatids (Figure 3A and Supplementary Figure S2A). Thus, ~31–33% of mutants missing *mir-44* and *mir-45* did not begin sperm formation until the late L4 stage, which is a greatly reduced time period for sperm formation. However,

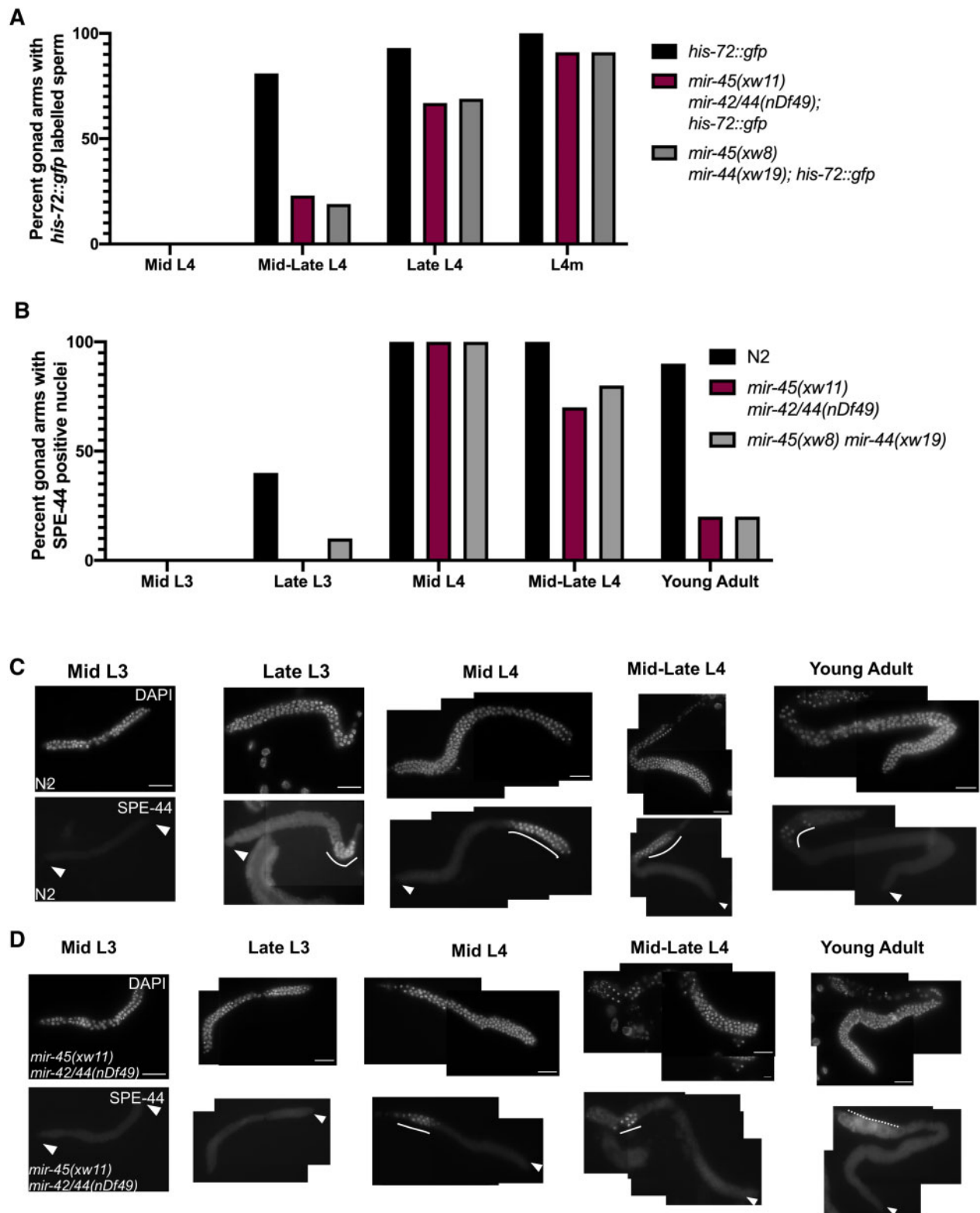


**Figure 3** *mir-44* and *mir-45* regulate the period of sperm production. (A) Percentage of gonad arms analyzed from worms with *his-72::gfp*-labeled sperm at each time point ( $n \geq 10$  per time point for each strain) for *his-72::gfp* control, *mir-45(xw11) mir-42/44(nDf49); his-72::gfp*, and *mir-45(xw8) mir-44(xw19); his-72::gfp* worms. (B) Percentage of gonad arms assayed at each time point with any SPE-44-labeled nuclei ( $n = 10$  per time point for each strain) for N2 control, *mir-45(xw11) mir-42/44(nDf49)*, and *mir-45(xw8) mir-44(xw19)*. Representative images of dissected germline arms labeled with an antibody for SPE-44 in wild-type N2 control (C) and *mir-45(xw11) mir-42/44(nDf49)* gonads (D). Images show DAPI (top) and anti-SPE-44 (bottom) labeling. Arrows indicate distal end of germline, solid lines indicate SPE-44 labeled cells, and dashed lines indicate oocytes. All images were captured with a 200 ms exposure. Scale bars equal 25  $\mu\text{m}$ . Details for staging worms are provided in Methods.

nearly all mutants with a loss of *mir-44* and *mir-45* do eventually show characteristic haploid spermatids by the L4m stage. These data are consistent with the brood size data and sperm quantification in which individual mutant worms showed variation in the total brood size and sperm number with some animals having very low brood sizes and others similar to the wild-type control (Figure 2A and G).

To molecularly assess if the timing of sperm specification is abnormal in mutants with the loss of *mir-44* and *mir-45*, we analyzed the expression of *spe-44* as a marker for sperm-specific transcription. *spe-44* is transiently expressed in germ cells that are being specified as sperm (Kulkarni et al. 2012). Using an anti-SPE-44 antibody, we determined when sperm cells are being specified in the gonad. In the N2 control, sperm begin to be specified at the late L3 stage when 30% (3/10 animals) had SPE-44-positive germ cells (Figure 3B and C). In later stages, from mid-L4 to young adult, all N2 control gonads had SPE-44-positive nuclei, indicating that cells are still being specified for sperm (Figure 3B and C). However, at the same late L3 timepoint, no (0/10) *mir-45(xw11) mir-42/44(nDf49)* mutants show SPE-44-positive germ cells and only 10% (1/10 animals) of *mir-45(xw8) mir-44(xw19)* mutants have SPE-44-positive germ cells indicating that the mutants have a delay in the initiation of sperm specification (Figure 3B and D and Supplementary Figure S2B). All mutants with the loss of *mir-44* and *mir-45* are specifying sperm by the mid-L4 stage. At the mid-late L4 stage, the number of SPE-44 positive gonads begins to decrease to 60% (6/10) and 70% (7/10) for *mir-45(xw11) mir-42/44(nDf49)* and *mir-45(xw8) mir-44(xw19)*, respectively, compared to the N2 control where all animals are still

specifying sperm. This indicates that some mutants with the loss of *mir-44* and *mir-45* have finished sperm specification prematurely (Figure 3B–D and Supplementary Figure S2B). Furthermore, by young adult, when 90% (9/10) of the N2 control still have SPE-44-positive cells, only 20% (2/10) of both the *mir-45(xw11) mir-42/44(nDf49)* and *mir-45(xw8) mir-44(xw19)* mutants have any SPE-44-positive cells. In fact, some mutants show oocyte formation in the young adult stage. This suggests that *mir-44* and *mir-45* function to regulate the timing of specification of germ cell fates since worms show both a delay and a premature termination of sperm specification along with earlier production of oocytes.

### *mir-45* is expressed in the hermaphrodite gonad arm during larval development

Previously published analysis of *mir-44* family expression using transgenes containing miRNA promoters driving GFP shows expression in various somatic tissues (Martinez et al. 2008). These transgenes were integrated into the genome using particle bombardment, which often leads to transgene silencing in the germline (Hunt-Newbury et al. 2007; Reece-Hoyes et al. 2007). Therefore, we performed the expression analysis of worms with the *xw8* CRISPR-generated GFP knock-in allele to analyze *mir-45* expression in the hermaphrodite germline (Figure 4). *mir-45* expression was first detected in hermaphrodite germ cells by the late-L3 stage (Figure 4D), the time at which sperm begin to be specified (reviewed in Kimble and Crittenden 2007). GFP expression from the *mir-45* transcriptional reporter was detected in the germline into adulthood. However, the stability of the GFP protein

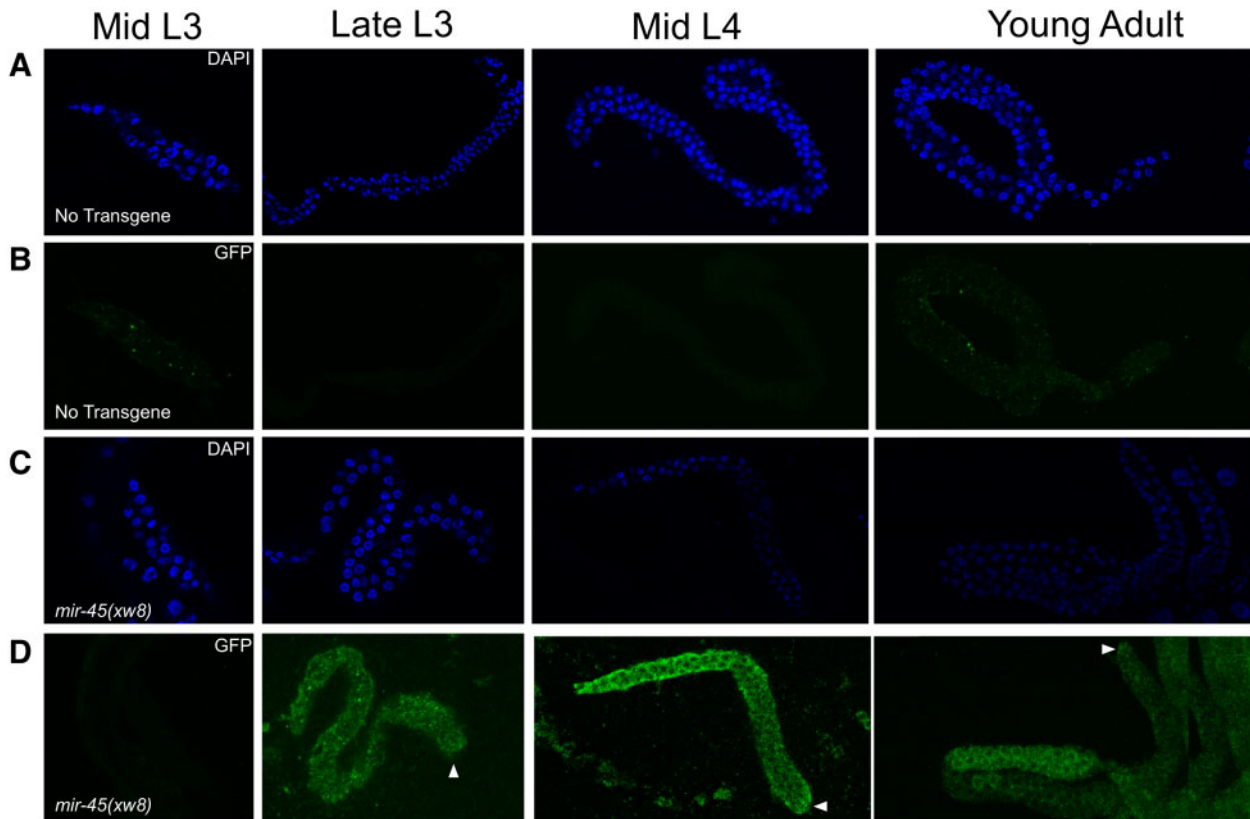


**Figure 4** *mir-45* is expressed in the hermaphrodite gonad arm. Developmental progression of *gfp* expression in *mir-45(xw8)* worms that have *gfp* inserted into the *mir-45* endogenous locus. Expression was analyzed in dissected germlines labeled with DAPI and an anti-GFP antibody. (A and B) Wild-type N2 worms, no transgene control. (C and D) *mir-45(xw8)* worms each with DAPI labeling (A and C) and anti-GFP labeling (B and D). Arrow indicates distal end of gonad arm ( $n = 10$  germlines analyzed per timepoint for each strain).



may preclude an accurate assessment of when *mir-45* expression stops. We did not detect *gfp* expression in either young adult *mir-45(xw8)* males (Supplementary Figure S3), which are actively specifying sperm or the no transgene controls in males and hermaphrodites (Supplementary Figure S3 and Figure 4B). The insertion of *gfp* in the *mir-44* locus (*xw6*) did not result in any detectable expression of *gfp* (data not shown), possibly due to nuclear processing of *mir-42* and *mir-43* from the pri-miRNA transcript, which could promote the degradation of the *gfp* sequence. Together, these data indicate that *mir-45* may be involved in the regulation of sperm specification in hermaphrodites but not males.

### ***mir-44* and *mir-45* regulate the pathway of germline sex determination**

Since mutants with the loss of *mir-44* and *mir-45* generate fewer sperm and show an early switch to oocyte production, we were interested in assessing genetic interactions with known regulators of the germline sex determination pathway. In hermaphrodites, specification of sperm and oocytes is tightly controlled by a complex set of regulators (reviewed in Ellis and Schedl 2007; Kimble and Crittenden 2007; Ellis 2008). Loss-of-function and gain-of-function mutations in this pathway of specification can alter the number of sperm produced (Barton et al. 1987; Crittenden et al. 2002; Thompson et al. 2005; Lamont and Kimble 2007). We first performed double mutant analysis between *mir-45(xw11) mir-42/44(nDf49)* mutants and mutants that disrupt germline sex determination, resulting in an over-production of sperm. We analyzed the genetic interaction of *mir-44* and *mir-45* with *fbf-1*, a critical regulator of spermatogenesis (Crittenden et al. 2002; Lamont et al. 2004). FBF-1 is an RNA-binding protein that binds targets in the 3' UTR and prevents the accumulation of target mRNAs in the mitotic region of the germline (Voronina et al. 2012). Loss-of-function *fbf-1(ok91)* mutants have an opposing phenotype to mutants with the loss of *mir-44* and *mir-45*, generating a significantly increased number of sperm and a later switch to producing oocytes than wild type (Crittenden et al. 2002). *mir-45(xw11) mir-42/44(nDf49); fbf-1(ok91)* mutants exhibited an increased number of sperm ( $377 \pm 79$ ,  $n = 10$ ), similar to what is observed in *fbf-1(ok91)* single mutants ( $416 \pm 90$ ,  $n = 11$ ; Figure 5A). While 10/15 *mir-45(xw11) mir-42/44(nDf49)* mutants showed early production of embryos, this defect was suppressed in *mir-45(xw11) mir-42/44(nDf49); fbf-1(ok91)* mutants, with only 1/14 showing early embryos (Supplementary Figure S4A). These data suggest that *mir-44* and *mir-45* may act upstream of *fbf-1* in the pathway for germline sex determination.

Since *fbf-1* functions at multiple steps in the pathway for germline sex determination, including functioning with both *fem-3* and *fog-1* (Zhang et al. 1997; Arur et al. 2011), we next analyzed the genetic interaction with *fem-3*. The downregulation of *fem-3* through FBF-1 binding in its 3' UTR is necessary for the switch to oogenesis (Ahringer and Kimble 1991; Zhang et al. 1997). *fem-3(q20gf)* gain-of-function mutants have a point mutation in the *fem-3* 3' UTR that interferes with its normal downregulation. *fem-3(q20gf)* mutants produce only sperm at the restrictive temperature and generate an increased number of sperm at the permissive temperature (Barton et al. 1987). We found that *mir-45(xw11) mir-42/44(nDf49); fem-3(q20gf)* mutants showed an over-production of sperm ( $340 \pm 76$ ,  $n = 11$  at 20°C) similar to the number of sperm in *fem-3(q20gf)* single mutants ( $394 \pm 122$ ,  $n = 10$  at 20°C) at the permissive or restrictive temperature (Figure 5B). In addition, *mir-45(xw11) mir-42/44(nDf49); fem-3(q20gf)* fail to make early embryos (Supplementary Figure S4B).

To further understand how *mir-44*, *mir-45*, and *fem-3* interact, we examined the *fem-3(q20gf)* sterility and Mog phenotypes. Mog worms only produce sperm and never switch to oogenesis and therefore produce no embryos. First, we examined the number of worms that produced no embryos in their reproductive lifetime. Both wild-type and *mir-45(xw11) mir-42/44(nDf49)* worms show no sterility or Mog phenotypes at 15 or 20°C (Table 1). At the intermediate temperature of 20°C, 12.9% of *fem-3(q20gf)* mutants were sterile. Whereas, surprisingly, 26.8% of *mir-45(xw11) mir-42/44(nDf49); fem-3(q20gf)* mutants were sterile. To ascertain if the sterile phenotype was due to Mog, we examined the number of Mog animals. At 20°C, 9.2% of *fem-3(q20gf)* mutants and 29.7% of *mir-45(xw11) mir-42/44(nDf49); fem-3(q20gf)* mutants displayed a Mog phenotype (Table 1). This was an unexpected result as mutants with the loss of *mir-44* and *mir-45* typically generate fewer sperm and switch to producing embryos early (Figure 2G and I). This result suggests a complex role for *mir-44* and *mir-45* in the process of germline sex determination.

Lastly, we tested the genetic interaction between *mir-44* and *mir-45* mutations and a *fog-1* loss-of-function allele. FOG-1 and FOG-3 are terminal regulators in the sperm specification pathway. FOG-1 and FOG-3 are necessary for the initiation of spermatogenesis and must subsequently be downregulated during L3 to allow for oogenesis to begin (Chen and Ellis 2000; Lamont and Kimble 2007). Loss of *fog-1* or *fog-3* results in a failure to produce sperm (Barton and Kimble 1990; Chen and Ellis 2000; Thompson et al. 2005). We examined *fog-1(q253)*, a reduced function temperature-sensitive mutant, which produces a reduced number of sperm at 20°C and no sperm at the restrictive temperature of 25°C. We observed an enhanced phenotype in *mir-45(xw11) mir-42/44(nDf49); fog-1(q253)* mutant worms at 20°C ( $50 \pm 42$ ,  $n = 10$ ) with significantly fewer sperm compared to *mir-45(xw11) mir-42/44(nDf49)* or *fog-1(q253)* controls ( $139 \pm 79$ ,  $n = 15$  and  $99 \pm 27$ ,  $n = 12$ , respectively; Figure 5C). In addition, *fog-1(q253)* mutants produced early embryos at 20°C consistent with an early sperm to oocyte switch. The early embryo phenotype was observed in 3/15 of *mir-45(xw11) mir-42/44(nDf49); fog-1(q253)* mutants compared to 10/15 of *mir-45(xw11) mir-42/44(nDf49)* and 10/15 *fog-1(q253)* mutants (Supplementary Figure S4C). This likely reflects the low number of sperm generated in *mir-45(xw11) mir-42/44(nDf49); fog-1(q253)* mutants resulting in few embryos (Figure 5C). This suggests that *mir-44* and *mir-45* may function to regulate *fog-1* or, alternatively, they may function in parallel to specify sperm.

To determine if *mir-44* and *mir-45* function upstream or in parallel to *fog-1*, we assessed FOG-1 protein levels using a rescuing 3xMyc tagged FOG-1 transgene (Noble et al. 2016) to compare expression in a Myc::FOG-1 control and *mir-45(xw11) mir-42/44(nDf49); Myc::FOG-1* mutant worms. We examined Myc::FOG-1 levels at multiple timepoints during development. In the control, Myc::FOG-1 is detected at mid-L3 and stays elevated through mid-L4 (Lamont and Kimble 2007; Noble et al. 2016; Figure 5D and E). However, in *mir-45(xw11) mir-42/44(nDf49)* mutants, the upregulation of FOG-1 is delayed with expression detected first at late L3 and persists into late L4 (Figure 5D and E). As the total period that FOG-1 is expressed in *mir-45(xw11) mir-42/44(nDf49)* mutants is decreased, this misregulation of FOG-1 is predicted to reduce the number of sperm produced (Lamont and Kimble 2007). Together, these data support a model that *mir-44* and *mir-45* may act to promote sperm production through the regulation of *fbf-1* and *fem-3* to allow for the normal expression of FOG-1 at the L3 stage (Figure 6A), although the precise mechanism whereby

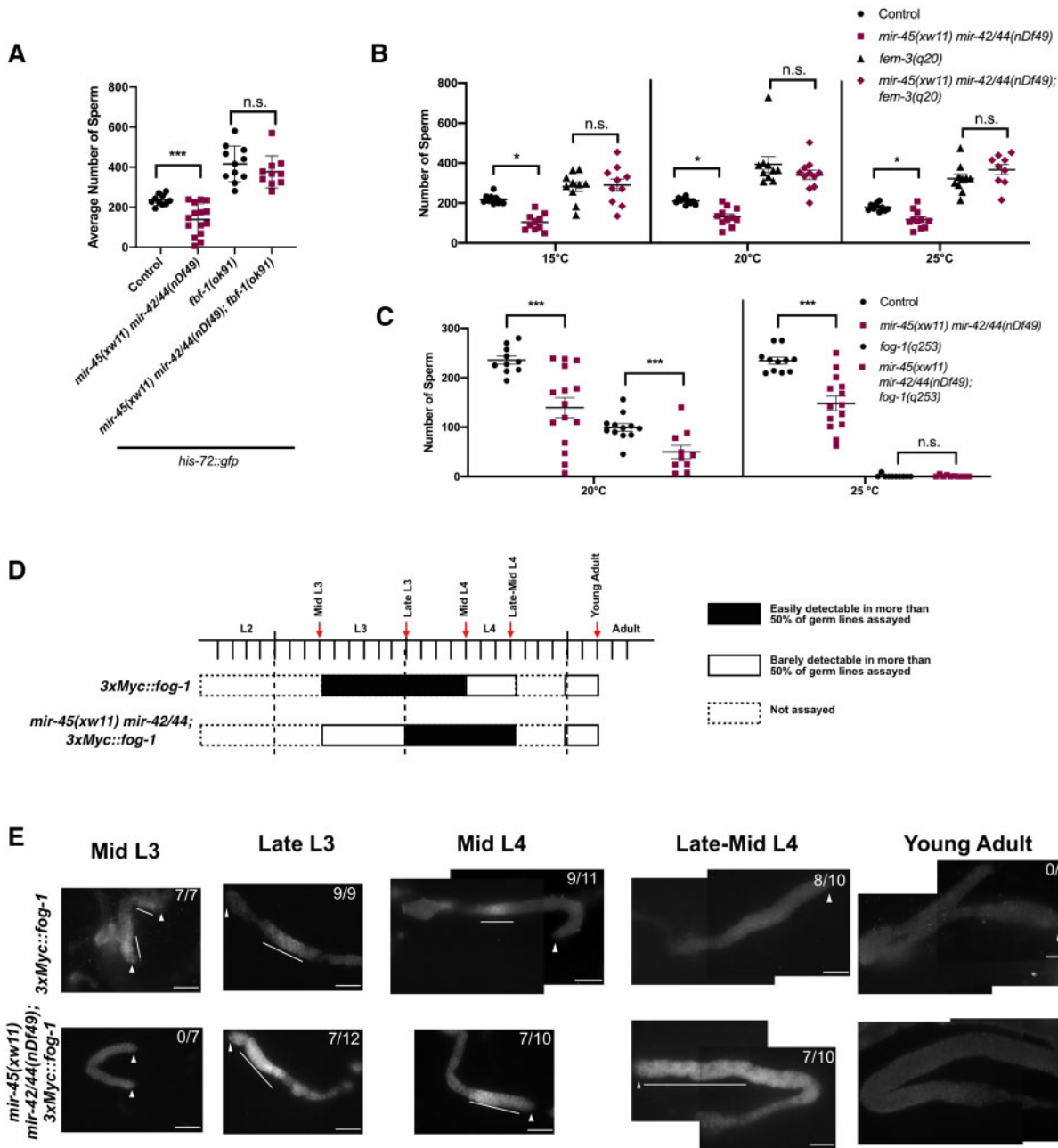


**Figure 5** *mir-44* and *mir-45* modulates the process of germline sex determination. (A–C) Quantification of sperm in individual hermaphrodites. All strains have *his-72::gfp* (*stIs10027*) in the background. (A) Analysis of genetic interactions with *fbf-1(ok91)*. Number of sperm in hermaphrodites at L4m + 5 h ( $n \geq 10$  for each strain). (B) Analysis of genetic interactions with *fem-3(q20gf)*. Number of sperm from young adults before any ovulation events ( $n \geq 10$  for each strain). Because *his-72::gfp* transgene expression in sperm was not detected in *fem-3(q20gf)* mutants, sperm quantification was performed using DAPI labeling in these strains. (C) Analysis of genetic interactions with *fog-1(q253)*. Number of sperm at L4m + 4 h at 20°C and L4m + 3 h at 25°C ( $n \geq 10$  for each strain). (D) Summary of temporal expression patterns observed in germlines scored for FOG-1 levels using the 3xMyc::FOG-1 transgene. Vertical lines along top indicate the number of hours post-molt. Red arrows correspond to timepoints assayed. Black highlighted regions indicate easily detectable levels of FOG-1. Dashed regions indicate germline timepoints not assayed. (E) Representative images of dissected germlines that express the 3xMyc::FOG-1 transgene. Arrows indicate distal end of the germline, white lines indicate region where staining was easily detected. Number in the upper right corner is the number of images captured with easily detectable FOG-1. All images captured with a 500 ms exposure time. Scale bars = 25  $\mu$ m. For graphs in (A)–(C), each marker represents data for a single worm with a line indicating average  $\pm$  SEM. One-way ANOVA followed by Tukey post hoc test: \* $P < 0.05$ , \*\*\* $P < 0.001$ , n.s. indicates  $P > 0.05$ .

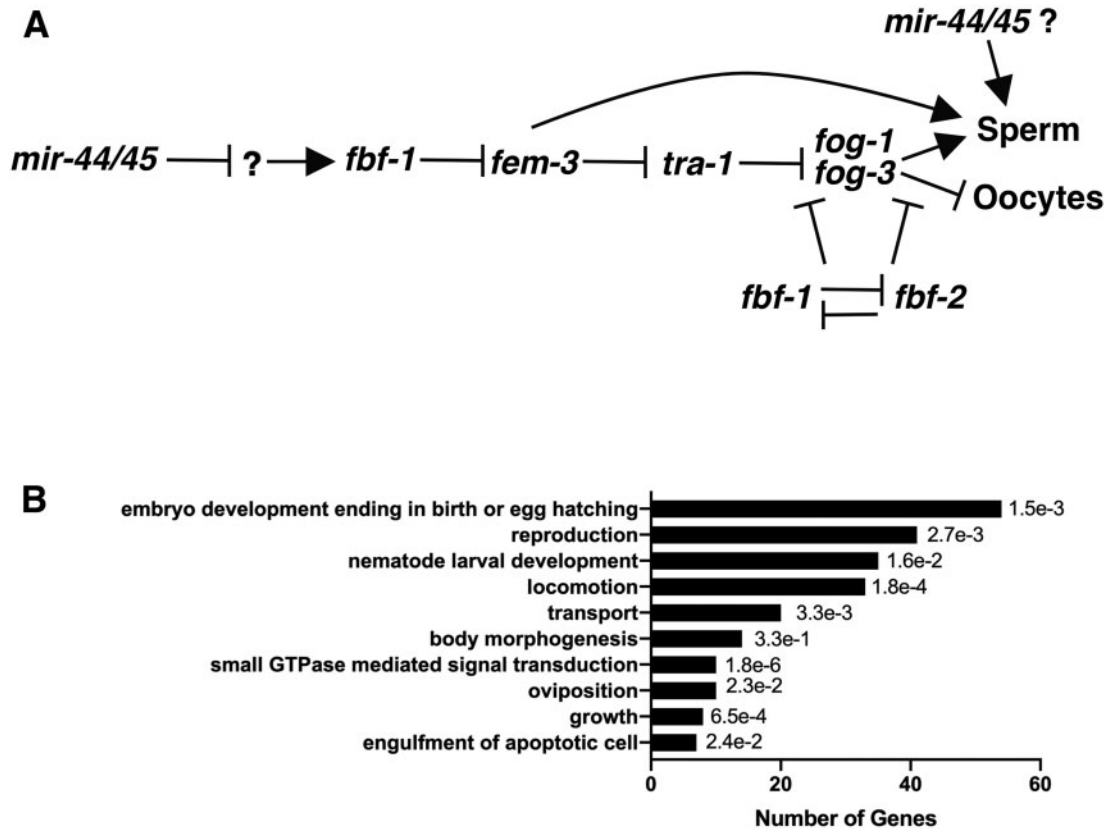
*mir-44* and *mir-45* regulates germline sex determination remains unknown.

miRNA target prediction algorithms do not identify any of the key regulators of the germline sex determination pathway as direct miR-44/45 targets including *fem-3*, *fbf-1*, and *fog-1*. Analysis of the 162 germline-expressed targets predicted by

the TargetScan algorithm (Jan et al. 2011; Supplementary Table S4) has found an enrichment in a number of GO terms including genes involved in reproduction, development, and small GTPase-mediated signaling (Figure 6B and Supplementary Table S5). Transcriptome analysis and biochemical approaches to identify direct targets will be needed to

**Table 1** Sterile and Mog phenotypes of *mir-45(xw11) mir-42/44(nDf49); fem-3(gf)* mutants

	Percentage of sterile animals		Percentage of Mog animals	
	15°C	20°C	15°C	20°C
Wild type	0% (0/93)	0% (0/98)	0% (0/76)	0% (0/79)
<i>mir-45(xw11)</i>	0% (0/92)	0% (0/101)	0% (0/62)	0% (0/85)
<i>mir-42/44(nDf49)</i>				
<i>fem-3(q20gf)</i>	1.2% (1/87)	12.9% (11/85)	0% (0/65)	9.2% (7/76)
<i>mir-45(xw11)</i>	5.2% (5/96)	26.8% (25/93)	1.6% (1/65)	29.7% (22/74)
<i>mir-42/44(nDf49); fem-3(q20gf)</i>				

**Figure 6** Model of *mir-44* and *mir-5* regulation of germline sex determination. (A) Simplified working models of the *mir-44* and *mir-5* regulatory network. *mir-44* and *mir-5* likely act to repress an unidentified factor that positively regulates *fbf-1* and coordinates the downstream specification of sperm or that *mir-44* and *mir-5* may can act on other mRNAs that regulate this process. (B) Highest GO terms of computationally predicted *mir-44* family germline targets. Numbers to the right represent P-values.

elucidate the network of targets controlled by the *mir-44* family of miRNAs.

## Discussion

These results identify a role for miRNAs in *C. elegans* hermaphrodites to promote sperm fate during larval development. While phenotypic analysis indicates that the four family members are all necessary for normal fecundity and the strongest defects are observed in mutants with loss of the complete *mir-44* family, additive effects are relatively modest and suggest complex roles for individual family members. Indeed, previous studies have shown that *mir-44* family members function antagonistically in the regulation of egg laying behavior, with *mir-44*, *mir-45*, and *mir-247*

mutants showing increased egg retention and *mir-61* mutants showing decreased egg retention (Alvarez-Saavedra and Horvitz 2010). Further analysis of these phenotypes could reveal distinct functions for other members of the *mir-44* family in the soma and germline. Distinct functions for individual family members likely reflect differences in spatial and temporal expression patterns as well as differences in the mature miRNA sequences that can lead to regulation of different mRNA targets.

Our evidence supports a model that the two identical family members, *mir-44* and *mir-45*, function together in the hermaphrodite germline during larval development to indirectly control key regulators of germline sex determination, including *fbf-1*, *fem-3*, and *fog-1*, to promote sperm specification and delay oocyte specification. These miRNAs promote the robust expression of the

sperm cell fate in a tightly controlled temporal window since we see a significant reduction in sperm production with a high degree of variability in the population of mutants with the loss of *mir-44* and *mir-45*. Mutants that lack *mir-44* and *mir-45* show variability in their brood size, sperm number, timing of sperm specification and production, and expression of FOG-1. This suggests that these miRNAs may function to reinforce the regulatory network that controls the sex determination pathway providing stability and robustness to the system (Raser and O'Shea 2005; Ebert and Sharp 2012).

Our data indicate that *mir-44* and *mir-45* promote sperm specification through regulation of the germline sex determination pathway, though specific mRNA targets have not yet been identified. Analysis of genetic interactions of mutants with the loss of *mir-44* and *mir-45* shows a complex relationship with several different genes involved in germline sex determination. First, *mir-44* and *mir-45* may function to promote the early rise and accumulation of FOG-1 during larval development. Mutants without these miRNAs show a delay in the period of FOG-1 expression, which correlates with a delay in sperm specification and spermatid production. However, analysis of the expression of FOG-1 in *mir-45(xw11) mir-42/44(nDf49)* mutants also suggests an extended period of expression into the mid-late L4 stage. Yet, this extended FOG-1 expression past the mid-L4 stage does not appear to be sufficient to maintain sperm production since the majority of these mutants do not show an extended window of sperm production but rather 67% show a premature switch to oocyte production. FOG-1 specification of sperm is dose dependent: high levels of FOG-1 promote sperm specification while lower levels of FOG-1 can encourage the proliferation of germ cells (Thompson et al. 2005). Thus, it is possible that there is an overall attenuation of FOG-1 activity in mutants missing *mir-44* and *mir-45*, which could result in L4-stage worms that express *fog-1* but, importantly, are below a threshold level of FOG-1 needed to maintain sperm production, thereby leading to an early switch to oogenesis in these mutant worms.

Second, *mir-44* and *mir-45* show a complex interaction with the *fem-3(q20gf)* allele. *fem-3(20gf)* and *mir-45(xw11) mir-42/44(nDf49)* have opposite effects on sperm production: *fem-3(q20gf)* mutants show excess sperm production while *mir-45(xw11) mir-42/44(nDf49)* mutants show reduced sperm production. *mir-45(xw11) mir-42/44(nDf49)*; *fem-3(q20gf)* mutants show essentially the same increase in the number of sperm produced by the young adult stage as *fem-3(q20gf)*. However, an unexpected result was that the loss of *mir-44* and *mir-45* enhanced the sterile phenotype and the Mog phenotype associated with *fem-3(gf)* mutants (Table 1). One possible observation that could account for this enhanced Mog phenotype is the observed extended window of expression of FOG-1 in *mir-45(xw11) mir-42/44(nDf49)* mutants. While this extended expression of FOG-1 is insufficient to drive an extended period of sperm production in *mir-45(xw11) mir-42/44(nDf49)* mutants, together with the *fem-3(q20gf)* mutation, which also increases FOG-1 levels, it may be sufficient to drive more worms over a threshold level needed to maintain sperm specification for a longer period of time in *mir-45(xw11) mir-42/44(nDf49)*; *fem-3(q20gf)* mutants (Table 1).

*mir-44* and *mir-45* could also function in parallel to FOG-1 and FOG-3, the known terminal regulators of this pathway. The *fem* genes have been shown to play an additional role in spermatogenesis since mutants in *fem*; *tra-1* genes, in which FOG-3 levels are high, only make oocytes, not sperm (Chen and Ellis 2000). The specific mechanism by which this occurs has not been established. Finally, if *mir-44* and *mir-45* act upstream of FBF-1 as the

genetic interaction data suggest, the possibility of interacting with many other mRNAs involved in spermatogenic and oogenic networks is likely since many sex-specific mRNAs have predicted FBF-binding sites (Porter et al. 2019). These results further reinforce both the complexity of this process and the many questions that need to be addressed about the mechanism whereby *mir-44* and *mir-45* act to promote a stable period of spermatogenesis in the hermaphrodite germline. *mir-44* and *mir-45* appear to function independently from another miRNA family that functions in the specification of sperm, the *mir-35* family (McJunkin and Ambros 2014, 2017). The *mir-35* family miRNAs are expressed earlier in development and the validated *mir-35* family target mRNAs, *sup-26* and *nhl-2*, are not predicted to be bound and regulated by the *mir-44* family. One member of the *mir-35* family, *mir-42*, is in a polycistronic cluster with *mir-43* and *mir-44*. Surprisingly, miR-42 and miR-43 levels in the *mir-45(xw8) mir-44(xw19)* mutant were significantly elevated relative to wild-type worms. It is possible that the 100 nucleotide deletion of *mir-44* coupled with insertion of a *gfp* coding sequence results in an increased amount of processed *mir-42/43* pre-miRNAs. In contrast, it remains possible that transcription of the pri-miRNA is enhanced in *mir-45(xw8) mir-44(xw19)* mutants. However, the strain with a deletion of *mir-42* had the same fecundity and sperm defects as the strain with elevated *mir-42* miRNA levels. This supports a conclusion that observed defects do not reflect the activity of the *mir-35* family member, *mir-42*. The primary fertility defects observed including reduced brood size, reduced sperm count, and early embryo production were comparable between *mir-45(xw8) mir-44(xw19)* and *mir-45(xw11) mir-42/44(nDf49)* despite having opposite effects on *mir-42* and *mir-43* activities.

The function for the *mir-44* family in the germline sex determination pathway is likely to be complex and require a detailed understanding of the *mir-44* family member's specific mRNA targets. A direct target for the *mir-44* family has not yet been identified. Examination of the list of potential *mir-44* family targets reveals many mRNA targets that could function upstream of *fbf-1* to regulate the germline sex determination pathway. For example, in the sexual reproduction GO terms *cye-1*, *rab-11.1*, and *ima-3* are identified, which all have roles in regulating meiosis in the germline. The misregulation of these targets could alter the downstream levels of *fbf-1*, *fem-3*, and *fog-1* (Geles and Adam 2001; Cheng et al. 2008; Mohammad et al. 2018). Interestingly, *mir-44* family homologs in *Drosophila* regulate Apontic in the stem cells of the testes to balance maintenance and differentiation (Monahan and Starz-Gaiano 2016). This is similar to our result where loss of *mir-44* and *mir-45* regulates the period where sperm are produced. The *Drosophila* target Apontic, which is a component of JAK-STAT signaling, does not have a *C. elegans* ortholog. The high degree of variability in penetrance of the defects observed in *mir-44* family mutants suggests that these miRNAs may act to modulate a network of mRNA targets that could function in shared pathways or processes to control germline sex determination in *C. elegans* hermaphrodites at the time of the sperm specification. This work describes a function for *mir-44* and *mir-45* in controlling the period of spermatogenesis in hermaphrodite larval development and identifies additional posttranscriptional regulation in the germline sex determination pathway.

## Acknowledgments

Some strains used in this study were obtained from the CGC, which is funded by NIH Office of Research Infrastructure



Programs (P40 OD010440). We thank Ron Ellis for his comments and discussion. We also thank members of the Abbott laboratory for their comments on the manuscript as well as the Kimble laboratory for sharing the *qSi140 [3xMyc::fog-1]* in a *fog-1(q785)* strain with us and Harold Smith for the SPE-44 antibody.

Conceptualization: K.A.M. and A.L.A.; investigation: K.A.M. and B.S.O.; resources: A.L.A.; writing—original draft: K.A.M. and A.L.A.; writing—review and editing: K.A.M. and A.L.A.; visualization: K.A.M.; formal analysis: K.A.M. and A.L.A.; funding acquisition: A.L.A.

## Funding

This work was supported by NIH grant number 1R15GM126458.

## Conflicts of interest

None declared.

## Literature cited

- Ahringer J, Kimble J. 1991. Control of the sperm-oocyte switch in *Caenorhabditis elegans* hermaphrodites by the *fem-3* 3' untranslated region. *Nature*. 349:346–348.
- Alvarez-Saavedra E, Horvitz HR. 2010. Many families of *C. elegans* microRNAs are not essential for development or viability. *Curr Biol*. 20:367–373.
- Ambros V, Ruvkun G. 2018. Recent molecular genetic explorations of *Caenorhabditis elegans* microRNAs. *Genetics*. 209:651–673.
- Amiri A, Keiper BD, Kawasaki I, Fan Y, Kohara Y, et al. 2001. An isoform of eIF4E is a component of germ granules and is required for spermatogenesis in *C. elegans*. *Development*. 128:3899–3912.
- Arur S, Ohmachi M, Berkseth M, Nayak S, Hansen D, et al. 2011. MPK-1 ERK controls membrane organization in *C. elegans* oogenesis via a sex-determination module. *Dev Cell*. 20:677–688.
- Bachorik JL, Kimble J. 2005. Redundant control of the *Caenorhabditis elegans* sperm/oocyte switch by PUF-8 and FBF-1, two distinct PUF RNA-binding proteins. *Proc Natl Acad Sci USA*. 102:10893–10897.
- Bartel DP. 2018. Metazoan microRNAs. *Cell*. 173:20–51.
- Barton MK, Kimble J. 1990. *fog-1*, a regulatory gene required for specification of spermatogenesis in the germ line of *Caenorhabditis elegans*. *Genetics*. 125:29–39.
- Barton MK, Schedl TB, Kimble J. 1987. Gain-of-function mutations of *fem-3*, a sex-determination gene in *Caenorhabditis elegans*. *Genetics*. 115:107–119.
- Bezler A, Braukmann F, West SM, Duplan A, Conconi R, et al. 2019. Tissue- and sex-specific small RNAomes reveal sex differences in response to the environment. *PLoS Genet*. 15:e1007905.
- Brown KC, Svendsen JM, Tucci RM, Montgomery BE, Montgomery TA. 2017. ALG-5 is a miRNA-associated Argonaute required for proper developmental timing in the *Caenorhabditis elegans* germline. *Nucleic Acids Res*. 45:9093–9107.
- Bukhari SIA, Vasquez-Rifo A, Gagné D, Paquet ER, Zetka M, et al. 2012. The microRNA pathway controls germ cell proliferation and differentiation in *C. elegans*. *Cell Res*. 22:1034–1045.
- Byerly L, Scherer S, Russell RL. 1976. The life cycle of the nematode *Caenorhabditis elegans*. II. A simplified method for mutant characterization. *Dev Biol*. 51:34–48.
- Casadaban MJ, Martinez-Arias A, Shapira SK, Chou J. 1983. Beta-galactosidase gene fusions for analyzing gene expression in *Escherichia coli* and yeast. *Method Enzymol*. 100:293–308.
- Chen P, Ellis RE. 2000. TRA-1A regulates transcription of *fog-3*, which controls germ cell fate in *C. elegans*. *Development*. 127:3119–3129.
- Cheng H, Govindan JA, Greenstein D. 2008. Regulated trafficking of the MSP/Eph receptor during oocyte meiotic maturation in *C. elegans*. *Curr Biol*. 18:705–714.
- Crittenden S, Kimble J. 2006. Immunofluorescence methods for *Caenorhabditis elegans*. In: Spector DL, Goldman RD, editors. *Basic Methods in Microscopy: Protocols and Concepts from Cells: A Laboratory Manual*. pp. 193–200.
- Crittenden SL, Bernstein DS, Bachorik JL, Thompson BE, Gallegos M, et al. 2002. A conserved RNA-binding protein controls germline stem cells in *Caenorhabditis elegans*. *Nature*. 417:660–663.
- Denli AM, Tops BBJ, Plasterk RHA, Ketting RF, Hannon GJ. 2004. Processing of primary microRNAs by the Microprocessor complex. *Nature*. 432:231–235.
- Dickinson DJ, Pani AM, Heppert JK, Higgins CD, Goldstein B. 2015. Streamlined genome engineering with a self-excising drug selection cassette. *Genetics*. 200:1035–1049.
- Duan H, de Navas LF, Hu F, Sun K, Mavromatakis YE, et al. 2018. The *mir-279/996* cluster represses receptor tyrosine kinase signaling to determine cell fates in the *Drosophila* eye. *Development*. 145:dev159053–13.
- Ebert MS, Sharp PA. 2012. Roles for microRNAs in conferring robustness to biological processes. *Cell*. 149:515–524.
- Ellis, R. and Schedl, T. 2007. Sex determination in the germ line (March 5, 2007), *WormBook*, ed. The *C. elegans* Research Community, *WormBook*, doi/10.1895/wormbook.1.82.2, <http://www.wormbook.org>.
- Ellis RE. 2008. Sex determination in the *Caenorhabditis elegans* germ line. *Curr Top Dev Biol*. 83:41–64.
- Friedman RC, Farh KKH, Burge CB, Bartel DP. 2008. Most mammalian mRNAs are conserved targets of microRNAs. *Genome Res*. 19:92–105.
- Fromm B, Billipp T, Peck LE, Johansen M, Tarver JE, et al. 2015. A uniform system for the annotation of vertebrate microRNA genes and the evolution of the human microRNAome. *Annu Rev Genet*. 49:213–242.
- Fromm B, Domanska D, Høye E, Ovchinnikov V, Kang W, et al. 2020. MirGeneDB 2.0: the metazoan microRNA complement. *Nucleic Acids Res*. 48:D132–D141.
- Geles KG, Adam SA. 2001. Germline and developmental roles of the nuclear transport factor importin alpha3 in *C. elegans*. *Development*. 128:1817–1830.
- Gervaise AL, Arur S. 2016. Spatial and Temporal Analysis of Active ERK in the *C. elegans* Germline. *J. Vis. Exp.* (117):e54901.
- Greenstein D. 2005. Control of oocyte meiotic maturation and fertilization (December 28, 2005), *WormBook*, ed. The *C. elegans* Research Community, *WormBook*, doi/10.1895/wormbook.1.53.1, <http://www.wormbook.org>.
- Grishok A, Pasquinelli AE, Conte D, Li N, Parrish S, et al. 2001. Genes and mechanisms related to RNA interference regulate expression of the small temporal RNAs that control *C. elegans* developmental timing. *Cell*. 106:23–34.
- Hodgkin JA, Barnes TM. 1991. More is not better: brood size and population growth in a self-fertilizing nematode. *Proc R Soc Lond B*. 246:19–24.
- Huang D-W, Sherman BT, Lempicki RA. 2009. Systematic and integrative analysis of large gene lists using DAVID bioinformatics resources. *Nat Protoc*. 4:44–57.
- Huang J, Wang H, Chen Y, Wang X, Zhang H. 2012. Residual body removal during spermatogenesis in *C. elegans* requires genes that mediate cell corpse clearance. *Development*. 139:4613–4622.

- Huggins HP, Subash JS, Stoffel H, Henderson MA, Hoffman JL, et al. 2020. Distinct roles of two eIF4E isoforms in the germline of *Caenorhabditis elegans*. *J Cell Sci* 133:jcs237990. doi: 10.1242/jcs.237990
- Hunt-Newbury R, Viveiros R, Johnsen R, Mah A, Anastas D, et al. 2007. High-throughput in vivo analysis of gene expression in *Caenorhabditis elegans*. *PLoS Biol*. 5:e237–17.
- Jan CH, Friedman RC, Ruby JG, Bartel DP. 2011. Formation, regulation and evolution of *Caenorhabditis elegans* 3'UTRs. *Nature*. 469: 97–101.
- Kimble J, Crittenden SL. 2007. Controls of germline stem cells, entry into meiosis, and the sperm/oocyte decision in *Caenorhabditis elegans*. *Annu Rev Cell Dev Biol*. 23:405–433.
- Kulkarni M, Shakes DC, Guevel K, Smith HE. 2012. SPE-44 implements sperm cell fate. *PLoS Genet*. 8:e1002678–14.
- Lamont LB, Crittenden SL, Bernstein D, Wickens M, Kimble J. 2004. FBF-1 and FBF-2 regulate the size of the mitotic region in the *C. elegans* germline. *Dev Cell*. 7:697–707.
- Lamont LB, Kimble J. 2007. Developmental expression of FOG-1/CPEB protein and its control in the *Caenorhabditis elegans* hermaphrodite germ line. *Dev Dyn*. 236:871–879.
- Lau NC, Lim LP, Weinstein EG, Bartel DP. 2001. An abundant class of tiny RNAs with probable regulatory roles in *Caenorhabditis elegans*. *Science*. 294:858–862.
- Lee MH, Ohmachi M, Arur S, Nayak S, Francis R, et al. 2007. Multiple functions and dynamic activation of MPK-1 extracellular signal-regulated kinase signaling in *Caenorhabditis elegans* germline development. *Genetics*. 177:2039–2062.
- Lewis BP, Burge CB, Bartel DP. 2005. Conserved seed pairing, often flanked by adenosines, indicates that thousands of human genes are microRNA targets. *Cell*. 120:15–20.
- Lim LP, Lau NC, Weinstein EG, Abdelhakim A, Yekta S, et al. 2003. The microRNAs of *Caenorhabditis elegans*. *Genes Dev*. 17: 991–1008.
- Livak KJ, Schmittgen TD. 2001. Analysis of relative gene expression data using real-time quantitative PCR and the 2- $\Delta\Delta$ CT method. *Methods*. 25:402–408.
- Martinez NJ, Ow MC, Reece-Hoyes JS, Barrasa MI, Ambros VR, et al. 2008. Genome-scale spatiotemporal analysis of *Caenorhabditis elegans* microRNA promoter activity. *Genome Res*. 18:2005–2015.
- McCarter J, Bartlett B, Dang T, Schedl T. 1999. On the control of oocyte meiotic maturation and ovulation in *Caenorhabditis elegans*. *Dev. Biol*. 205:111–128.
- McEwen TJ, Yao Q, Yun S, Lee C-Y, Bennett KL. 2016. Small RNA in situ hybridization in *Caenorhabditis elegans*, combined with RNA-seq, identifies germline-enriched microRNAs. *Dev. Biol*. 418: 248–257.
- McJunkin K, Ambros V. 2014. The embryonic mir-35 family of microRNAs promotes multiple aspects of fecundity in *Caenorhabditis elegans*. *G3 (Bethesda)*. 4:1747–1754.
- McJunkin K, Ambros V. 2017. A microRNA family exerts maternal control on sex determination in *C. elegans*. *Genes Dev*. 31: 422–437.
- Merritt C, Rasoloson D, Ko D, Seydoux G. 2008. 3' UTRs are the primary regulators of gene expression in the *C. elegans* germline. *Curr Biol*. 18:1476–1482.
- Miller MA, Ruest PJ, Kosinski M, Hanks SK, Greenstein D. 2003. An Eph receptor sperm-sensing control mechanism for oocyte meiotic maturation in *Caenorhabditis elegans*. *Genes Dev*. 17:187–200.
- Minogue AL, Tackett MR, Atabakhsh E, Tejada G, Arur S. 2018. Functional genomic analysis identifies miRNA repertoire regulating *C. elegans* oocyte development. *Nat Commun*. 9:3–11.
- Miska EA, Alvarez-Saavedra E, Abbott AL, Lau NC, Hellman AB, et al. 2007. Most *Caenorhabditis elegans* microRNAs are individually not essential for development or viability. *PLoS Genet*. 3:e215–e219.
- Mohammad A, Vanden Broek K, Wang C, Daryabeigi A, Jantsch V, et al. 2018. Initiation of meiotic development is controlled by three post-transcriptional pathways in *Caenorhabditis elegans*. *Genetics*. 209:1197–1224.
- Monahan AJ, Starz-Gaiano M. 2016. Apontic regulates somatic stem cell numbers in *Drosophila* testes. *BMC Dev Biol*. 16:3044.
- Noble DC, Aoki ST, Ortiz MA, Kim KW, Verheyden JM, et al. 2016. Genomic analyses of sperm fate regulator targets reveal a common set of oogenic mRNAs in *Caenorhabditis elegans*. *Genetics*. 202:221–234.
- Porter DF, Prasad A, Carrick BH, Kroll-Connor P, Wickens M, et al. 2019. Toward identifying subnetworks from FBF binding landscapes in *Caenorhabditis* spermatogenic or oogenic germlines. *G3 (Bethesda)*. 9:153–165.
- Raser JM, O'Shea EK. 2005. Noise in gene expression: origins, consequences, and control. *Science*. 309:2010–2013.
- Reece-Hoyes JS, Shingles J, Dupuy D, Grove CA, Walhout AJM, et al. 2007. Insight into transcription factor gene duplication from *Caenorhabditis elegans* Promoterome-driven expression patterns. *BMC Genomics*. 8:27.
- Rios C, Warren D, Olson B, Abbott AL. 2017. Functional analysis of microRNA pathway genes in the somatic gonad and germ cells during ovulation in *C. elegans*. *Dev Biol*. 426:115–125.
- Ruby JG, Jan C, Player C, Axtell MJ, Lee W, et al. 2006. Large-scale sequencing reveals 21U-RNAs and additional microRNAs and endogenous siRNAs in *C. elegans*. *Cell*. 127:1193–1207.
- Thompson BE, Bernstein DS, Bachorik JL, Petcherski AG, Wickens M, et al. 2005. Dose-dependent control of proliferation and sperm specification by FOG-1/CPEB. *Development*. 132:3471–3481.
- Tzur YB, Winter E, Gao J, Hashimshony T, Yanai I, et al. 2018. Spatiotemporal gene expression analysis of the *Caenorhabditis elegans* germline uncovers a syncytial expression switch. *Genetics*. 210:587–605.
- Voronina E, Paix A, Seydoux G. 2012. The P granule component PGL-1 promotes the localization and silencing activity of the PUF protein FBF-2 in germline stem cells. *Development*. 139: 3732–3740.
- Ward JD. 2015. Rapid and precise engineering of the *Caenorhabditis elegans* genome with lethal mutation co-conversion and inactivation of NHEJ repair. *Genetics*. 199:363–377.
- Yoo AS, Greenwald I. 2005. LIN-12/Notch activation leads to microRNA-mediated down-regulation of Vav in *C. elegans*. *Science*. 310:1330–1333.
- Yoon WH, Meinhardt H, Montell DJ. 2011. miRNA-mediated feedback inhibition of JAK/STAT morphogen signaling establishes a cell fate threshold. *Nat Cell Biol*. 13:1062–1069.
- Zhang B, Gallegos M, Puoti A, Durkin E, Fields S, et al. 1997. A conserved RNA-binding protein that regulates sexual fates in the *C. elegans* hermaphrodite germ line. *Nature*. 390:477–484.